Strategies for Nested and Eddy-Resolving State Estimation

GEOFFREY GEBBIE[1,2*], PATRICK HEIMBACH[2], AND CARL WUNSCH[2]

1. Massachusetts Institute of Technology / Woods Hole Oceanographic Institution Joint Program,

2. Dept. of Earth, Atmospheric and Planetary Sciences, Massachusetts Institute of Technology,

Cambridge, MA, USA

Corresponding author address:

Geoffrey Gebbie, *Now at: Dept. of Earth and Planetary Sciences, Harvard University, 20 Oxford St., Cambridge, MA 02138, USA, (gebbie@eps.harvard.edu)

ABSTRACT

Both ocean process studies and oceanographic prediction studies will increasingly rely on state estimates (or data assimilation) as our most complete knowledge of what the ocean actually does. This study aims to apply the formalism and methodology of rigorous state estimation, recently developed for the global, coarse-resolution problem, to eddy-resolving state estimation in regional domains. Two major challenges exist for a state estimate that is nested inside a global state estimate: 1) control and estimation of open boundary conditions, and 2) the estimation of eddy-resolving initial conditions that lead to a desired model trajectory over yearly timescales. In this study, a carefully-posed least-squares cost function defines the problem of minimizing the misfit between a North Atlantic regional general circulation model and observations taken by the TOPEX/POSEIDON satellite altimeter and the Subduction Experiment field campaign. The use of the adjoint model of both an eddy-resolving adjoint model and its coarse-resolution twin leads to at least one solution to the least-squares problem in a computationally-practical way. Therefore, no fundamental obstacle exists to constrain a model nested within a large-scale circulation that is consistent with observations. A second experiment with the North Atlantic regional model also shows that individual eddy trajectories can be determined insofar as they are observed. The result of this study is a state estimate which is consistent with observations, self-consistent with the equations of motion, and one which explicitly resolves eddy-scale motions within a regional grid. One use for the regional state estimate is to diagnose regional processes, such as subduction rates, volume budgets, and buoyancy budgets, in a physically-interpretable context, and is completed in a companion paper.

1. Introduction

The statistical combination of observations and a numerical model, termed “state estimation” (or in the specialized meteorological context, “data assimilation”), provides a way to reconstruct the realistic time-evolving, three-dimensional circulation of the ocean—combining the newly-available global ocean data sets with the best of modern numerical general circulation models. Recent advances, such as those of the ECCO (Estimating the Circulation and Climate of the Ocean) Group (Fukumori 2002; Stammer et al. 2002, 2003, 2004) , demonstrate the practicality of state estimation in global, coarse-resolution ocean models. The forbidding high-dimensionality of the problem due to the large number of degrees of freedom in fluid flows, even at 1 or 2 degree spatial resolution, does not prove to be a fundamental obstacle. Although these previous results are promising, oceanographers still face a large variety of regional problems, such as those outlined by the CLIVAR and GODAE international research programs, and the next step is to apply global methods to regional state estimation. For regional state estimates with state-of-the-art general circulation models, two major problems must be tackled: 1) the estimation of a state estimate nested inside another state estimate, and 2) the estimation of the ocean circulation at eddy-resolution.

In regional problems, an adequate knowledge of the surrounding global ocean is required to avoid introducing errors owing to the particular area under study. In atmospheric models, the open boundaries are typically pushed far from the region of interest so that the details of the boundary do not affect the focus of study. Such an approach is not tractable in ocean models because the spatial scale of eddy motions is much smaller; hence, the extension of a computational domain incurs great additional cost. Fortunately for ocean modelers, a new era of global state estimates now provides knowledge of open-ocean density and velocity fields which can be used as open boundary conditions in a regional setting. At this early stage, such fields are highly uncertain. A useful product will explicitly account for such sources of uncertainty while estimating the regional circulation.

A prerequisite for a regional state estimate is a regional model simulation which gives a reasonable physical description. State-of-the-art numerical models solve the so-called primitive

equations, but the open boundary conditions in such models are a subject of ongoing research. One difficulty is the the computational need to fully impose the open boundary conditions in a general circulation model. In practice, the consistency of these open boundary conditions to the interior circulation can not be guaranteed *a priori*. Therefore, regional GCM simulations are formally overdetermined. Investigators such Marchesiello et al. (2001) have previously attacked this problem by proposing physically-based improvements to the open-boundary formulation which allow the interior circulation to modify the boundary conditions. These approaches will be needed in the future, but for the present, we note that inverse methods have already been developed to deal with overdetermined problems. The machinery of state estimation, for example, reduces to a form of least-squares problem in almost all practical applications. Specifically, state estimation problems minimize the squared data-model misfit. The open boundary conditions are treated as uncertain and subject to modification through the information contained in the interior of the domain. Conceptually, state estimation techniques handle the ill-posedness of regional simulations, but careful formulation of the least-squares problem is necessary.

Another challenge in regional state estimation is due to model resolution. Given realistic concerns over the errors incurred by failure to resolve major features of the flow and corresonding scalar fields, one seeks to obtain much higher resolution in specific oceanic regions. The study of ocean processes will also be enhanced by the availability of regional state estimates. In regional studies, the smaller domain size allows models to be run at higher resolution. Higher resolution ocean models are numerically stable with lower values of viscosity, and therefore, have higher and more realistic Reynolds numbers. Unfortunately, the spatial resolution usable for state estimates remains restricted in practice. Ultimately, one expects that increasing computing power and clever numerics will permit global calculations at ever-increasing resolution, but for the next decade at least, it appears that model and system resolution will remain well below desirable levels. In the near future, therefore, one wishes to know exactly what the restrictions are, and if there are any simple ways to extend the methodology.

The purpose of this paper is to further develop the methodology for state estimation of models with high regional resolution, employing a wide variety of data, as well as using information propagated through the open boundary from the oceanic state outside the highly resolved region.

Careful formulation of the open boundary problem is the subject of Section 2. A means for extending state estimation methods for eddy-resolving models is discussed in Section 3. In a regional setting, both open boundary estimation and eddy-resolving estimation are usually needed, but the methodologies of Sections 2 and 3 are largely independent, and could be applied to separate problems. Because application to a specific, realistic, case makes it simplest to describe the methodology, we will focus on the Subduction Experiment of the Northeast Atlantic Ocean (Brink et al. 1995), as described in Section 4. Because our machinery enables the calculation of an improved state estimation in the Subduction region, the opportunity is taken to reanalyze that experiment, and in particular to produce new estimates of subduction rates and variability in that area. But the focus of the present paper is primarily on the methodology, and most of the scientific analysis is postponed to a second companion paper (Gebbie, in preparation,2005).

2. Nesting a regional state estimate

Regional state estimation is the combined use of a regional simulation driven by boundary conditions from a global state estimate and regional observations. The formulation of our regional state estimate therefore depends upon a global state estimate, which we presume exists beforehand. New global state estimates, such as those of the ECCO Group (Stammer et al. 2003, 2004) make regional state estimation a realizable goal now.

As with any other form of state estimation, regional state estimation requires a numerical model which predicts the ocean state, $\mathbf{x}(t)$, where t is time. The *state vector* is defined to contain precisely that information, when supplemented by boundary conditions, required to step the model one time step, Δt into the future (we use the notation and terminology of Wunsch, 1996). Thus the model code computes,

$$\mathbf{x}(t+\Delta t) = \mathcal{L}[\mathbf{x}(t), \mathbf{Bq}(t), \Gamma\mathbf{u}(t)], \tag{1}$$

where $\mathbf{Bq}(t)$ represents surface forcing, boundary conditions, as well as internal model parameters (e.g., mixing coefficients), and $\Gamma\mathbf{u}(t)$ corresponds to all elements of the model that are subject to adjustment, including the initial conditions, surface flux adjustments and corrections to internal parameters. The vector $\mathbf{u}(t)$ is usually called the *control vector*, or simply the controls. Here,

operator $\mathcal{L}(\cdot)$ is a large, nonlinear computer code for regional simulations.

A second prerequisite for regional state estimation is a series of measurements within that region, $\mathbf{y}(t)$, which are usually a linear combination of the state vector, $\mathbf{y}(t) = \mathbf{E}(t)\mathbf{x}(t) + \mathbf{n}(t)$, where $\mathbf{n}(t)$ is the vector of inevitable, and non-zero, observation errors. The model-data misfit is then measured as,

$$J = \Sigma_{t=0}^{t_f} [\mathbf{E}(t)\mathbf{x}(t) - \mathbf{y}(t)]^T \, \mathbf{W}(t) \, [\mathbf{E}(t)\mathbf{x}(t) - \mathbf{y}(t)], \tag{2}$$

where $\mathbf{W}(t)$ is a weighting matrix most commonly, but not necessarily, the inverse of noise covariance matrix $\mathbf{R}(t) = \left\langle \mathbf{n}(t)\,\mathbf{n}(t)^T \right\rangle$, where the mean, $\langle \mathbf{n}(t) \rangle = 0$. Brackets denote expected value. *J* is usually called the "objective" or "cost" function. The investigator seeks the circulation that minimizes *J* until the misfit is acceptable, subject to Eq. (1) remaining valid.

a. Resolving the ill-posedness of the forward model

In a primitive equation model, the number of boundary conditions demanded computationally is irrespective of whether the boundary is open or closed. In all cases, the entire state, which includes temperature, salinity, and the two horizontal components of velocity, must be provided on the open boundaries, and therefore, appended to $\mathbf{q}(t)$ in Eq. (1). In closed boundary problems, the circulation usually adjusts to the boundary conditions by forming boundary layers. In the open boundary case, boundary layers are unphysical because no boundary layers exist in the open ocean. Therefore, the imposed open boundary conditions must be consistent with the interior circulation, something that is impossible to specify *a priori*. Formally, the forward model is overdetermined and hence, an ill-posed mathematical problem (Bennett and Kloeden 1981; Oliger and Sundström 1978).

With the advent of global state estimates, a first-guess for all components of $\mathbf{q}(t)$ is now available, e.g. $\mathbf{q}(t) = f(\tilde{\mathbf{x}}_{global}(t))$, where the function f maps global state estimate values, $\tilde{\mathbf{x}}_{global}(t)$, to the region. The global state estimate is necessarily imperfect, and therefore, the open boundary conditions should be treated as adjustable parameters. If one considers that the open boundary conditions consist of both a first-guess component, $\mathbf{q}_{ob}(t)$, and an unknown component, $\mathbf{u}_{ob}(t)$, which must be solved for, then the overdetermined forward model problem becomes an

underdetermined problem. For a nonlinear model, such as most general circulation models, there can be no proof that this inverse problem is well-posed, but we can always solve the corresponding least-squares problem and then analyze the solution for physical sense.

b. Formulation of the open boundary estimation problem

We have not yet mentioned the form of the control vector, $\mathbf{u}(t)$ in Eq. (1). Before state estimates were available, only open-ocean temperatures and salinities were easily accessible through climatological datasets such as those of Levitus and Boyer (1994). Consequently, investigators such as Stevens (1991) used the thermal wind relation to diagnose the open boundary velocities from the imposed density structure. This idea can be extended to the open boundary estimation problem by defining the control vector as the temperature and salinity on the open boundary, $\mathbf{u}_{ob}(t) = [\mathbf{T}_{ob}(t); \mathbf{S}_{ob}(t)]^T$, and then designing Γ such that it maps the temperature and salinity onto velocity via the thermal wind relationship. In practice, unfortunately, the thermal wind mapping is noisy, and it does not give any information on the depth-independent component of the flow.

Instead, the control vector can be set to the entire open boundary state, e.g., $\mathbf{u}_{ob}(t) = [\mathbf{T}_{ob}(t); \mathbf{S}_{ob}(t); \mathbf{V}_{\|}(t); \mathbf{V}_{\perp}(t)]^T$, where $\mathbf{V}_{\|}(t)$ is the horizontal component of velocity tangential to the open boundary, and $\mathbf{V}_{\perp}(t)$ is the normal component into the boundary. Then, the number of open boundary controls is equal to the number of computational boundary conditions. Thermal wind balance can be imposed by appending an extra term to the cost function in which a deviation from the dynamical balance is penalized. The extra term is sometimes called a *soft constraint*. In this case, thermal wind balance at the open boundary is: $\partial V_{\perp}/\partial z = -g/(\rho_0 f) \cdot \partial \rho/\partial x$, where x is the along-boundary coordinate, z is the depth coordinate, g is gravity, ρ is density with some reference value ρ_o, and f is the Coriolis parameter. Rearranging, this can be written as: $F(x,z) = \partial V_{\perp}/\partial z + g/(\rho_0 f) \cdot \partial \rho/\partial x = 0$. For the numerical model, a discrete version of $F(x,z)$ must be found (see Gebbie, Ph. D. thesis, for such a discretization). For the entire open boundary at all times, append values of $F(x,z)$ into vector form, $\mathbf{F} = [F(1,1), F(2,1) \ldots\ F(x_{max}, z_{max})]^T$. The additional term to the cost function then takes the form of a weighted squared deviation: $\mathbf{F}^T\mathbf{W}\mathbf{F}$ with $\mathbf{W}$ as a weighting matrix. Deviations from thermal wind are proportional to the

Rossby number, so the weighting term can be set with this physical guidance.

The choice of the entire open boundary state as a control vector allows the state estimation process to find the complete open boundary condition without restriction, but such a formulation leads to practical problems in the optimization process. When Ferron and Marotzke (2003) estimated this control vector in an Indian Ocean regional model, a two-step estimation process was necessary: one step to estimate the initial conditions and surface forcing, and a second step to estimate the open boundary conditions. One possible explanation for the necessity of a two-step approach is ill-conditioning of the control space. Physically, the search space is ill-conditioned when the interior circulation is highly sensitive to some control variations and relatively insensitive to other variations. With a regional model, consider the sensitivity of the sea surface height to the open boundary velocity. By conservation of volume, the sea surface reacts to a mean inflow by the relation: $d\overline{\eta}/dt = A_{xz}/A_{xy} \cdot \overline{V}_{\perp}$, where $\overline{\eta}$ is the regional-mean sea surface height, A_{xz} is the cross-sectional area of the open boundary, A_{xy} is the sea surface area, and $\overline{V}_{\perp}$ is the regional-mean velocity normal to the open boundary. In a square region with 1000 *km* sides, this scaling means that an imbalance of 1 mm/s causes the entire sea surface to rise by 1 *m* in approximately 12 days, which is unobserved in the ocean. The sensitivity of the domain-integrated sea surface height to the open boundary velocity is many orders of magnitude larger than any other physically-based sensitivities in the ocean.

The ill-conditioning in the control space of the open boundary velocity is resolved by redefining and rescaling the control vector $\mathbf{u}(t)$ in a way that is analogous to column scaling in linear algebra. We propose that the normal component of open boundary velocity be decomposed as such:

$$V_{\perp}(x,z) = V_1(x,z) + V_2(z) + V_3, \tag{3}$$

where V_1 is the depth-varying component of velocity, V_2 is the depth-independent component, and V_3 is a constant. These different components of the velocity field are expected to have different magnitudes, and after they are decomposed, can be individually scaled. In the present form, however, a particular normal velocity field may have more than one representation in terms of V_1, V_2, and V_3; the decomposition is degenerate because extra degrees of freedom were added. As a

remedy, force the depth-dependent velocity to have no net inflow in any column,

$$\Sigma_{z=1}^{H} V_1(x,z) \cdot \Delta z = 0, \tag{4}$$

where Δz is the thickness of a model level, H is the total depth of the ocean, and the equation holds at all gridpoints along the boundary. Furthermore, force the depth-independent velocity to have no net inflow into the regional domain:

$$\Sigma^{ob} V_2(x) \cdot \Delta x \cdot H(x) = 0, \tag{5}$$

where Δx is the length of the gridcell along the open boundary. For V_3, two choices remain. V_3 represents the scaled net volume flux into the domain, which should be nearly zero, although recent papers have called such an assumption into question (Fu et al. 2001; Wunsch and Gill 1976). The ideal case is let V_3 vary within an expected range and to estimate it. A second approach is to add a hard constraint to force the net volume flux into the basin to be zero, namely $V_3 = 0$, which makes the optimization problem easier to solve. The tradeoff is that one estimable quantity is lost.

c. Summary of nested state estimation

In summary, regional state estimation demands a particular form of the control vector. In our study, we take the control parameters that are used in the global problem, and append the following open boundary controls:

$$\mathbf{u}_{ob}(t) = [\mathbf{T}_{ob}(t); \mathbf{S}_{ob}(t); \mathbf{V}_{\|}(t); \mathbf{V}_1(t); \mathbf{V}_2(t)]^T. \tag{6}$$

Furthermore, we have appended the constraint of $V_3 = 0$, or a net balanced volume flux through the boundaries, to the model, to resolve any ill-conditioning of the search space. Finally, we have added a soft constraint to the cost function which penalizes any deviation from thermal wind balance, so that the estimated open boundary conditions are constrained to be physically reasonable.

Nested state estimation solves the previously difficult problem of finding adequate open boundary conditions in the open ocean by using a global state estimate. A nested state estimate is more than a nested simulation because it also uses regional observations to get the best estimate of what the ocean actually does. Information comes from outside the domain into the region of interest through the boundary conditions – but the interior observations are also used to update the boundary conditions. Therefore, there is a two-way information flow and all the available information is used to create the regional state estimate.

3. State estimation at eddy-resolution

The oceanographic state estimation problem is a giant, nonlinearly-constrained least-squares problem, and is advantageously solved using the formalism of the method of Lagrange multipliers, as reviewed by Wunsch (1996) and Bennett (2002). The method is sometimes called the "adjoint" method, (Hall et al. 1982; Sirkes et al. 1996) and *4D-VAR* (Talagrand 1997) in meteorological applications (where the control vector is restricted). The nonlinearity and large-dimensionality of the problem require an iterative search for a solution, as outlined by Marotzke et al. (1999). The search proceeds as a gradient-descent problem – similar to the search for the deepest valley in a high-dimensional mountain range. The topology of the search space depends upon the degree of nonlinearity in the model; quasi-linear models give a paraboloidal shapes, but for more nonlinear models, there is no guarantee that the topology of the cost function is globally concave. The emergence of many local minima in a cost function is a troublesome scenario, as gradient search methods do not distinguish between local and global minima.

Previous investigators found limitations of the adjoint method with eddy-resolving models. Tanguay et al. (1995) showed that geophysical turbulence models are increasingly nonlinear with integration time . Studies with eddy-resolving models of the North Atlantic(Cong et al. 1998; Köhl and Willebrand 2003; Morrow and Demey 1995; Schröter et al. 1993) found a maximum time window of a few months for successful combination of model and observations. A related problem was seen in sensitivity studies that employed an eddy-resolving adjoint model; Lea et al. (2000) showed that sensitivities calculated from an adjoint model differ from the "macroscopic climate sensitivity" - the sensitivity which emerges from finite perturbations. For these reasons,

the use of the method of Lagrange multipliers remains restricted to sufficiently-linear models, which serves as a restriction on the time-interval of estimation for a given resolution of model.

a. A multiscale method

In light of the seeming inevitability of local minima in the cost function computed by an eddy-resolving model, our strategy will be to start with a first guess that is as good as possible. A good starting point for solving the least-squares problem is already available: the ECCO 2° global state estimate. The 2° estimate can be further improved by forming a coarse-resolution regional state estimate which differs by using a regional model with open boundaries, and can differ by including regional data sets in the cost function. The best regional coarse-resolution estimate can then be used as a first guess in the regional eddy-resolving problem. This incremental approach, sometimes called a *multiscale method*, is computationally efficient because iterations of the search procedure can be done cheaply at coarse-resolution, which reduces the costly iterations at eddy resolution. Furthermore, state estimation with a coarse-resolution ocean model avoids many of the problems of an eddy-resolving estimation because the model is quasi-linear and the control space is much smaller.

In the multiscale method, one wishes to define the same cost function for both the coarse and eddy resolution problems. To be physically consistent, however, the cost function weights must be reconsidered at each resolution. The cost function is weighted such that its expected value is one when the large-scale circulation is consistent with the observations. The coarse-resolution model does not resolve motions at scales less than the grid spacing, and such information in the observations is not expected to be fit. The observations could be pre-filtered to only include the large-scale signal. Instead, the least-squares formulation is used to handle such a situation; the small-scale signal in the observations is considered noise. The weights are set to be inversely proportional to the expected noise, and are therefore decreased. The expected noise can be computed in the wavenumber band of interest via any independent model, such as the spectrum of Zang and Wunsch (2001). The eddy-resolution problem proceeds similarly – the small-scale observational signal is still considered noise. In addition, the eddy-resolving model predicts an eddy field which can not be expected to match the observations. Therefore, the total expected

error is the sum of both the small-scale observational signal and the model variability at those scales, and the chosen weights are chosen accordingly.

b. Summary of eddy-resolving state estimation

In light of the difficulties seen by previous investigators with eddy-resolving models, this study suggests a basic plan to search for an eddy-resolving state estimate:

1. Calculate the appropriate weights for the cost function such that the model circulation is only constrained to the large scale.

2. Find a best-guess circulation for the regional model by first optimizing the circulation in a coarse-resolution twin.

3. Apply the coarse-resolution estimate to the eddy-resolving run and continue optimization by the adjoint method until the eddy-resolving model is within observational uncertainty.

4. The Model Setup

The eastern subtropical North Atlantic Ocean is a favorable location for trials with regional state estimation for two major reasons. One, the region was host to an intensive field campaign to collect oceanographic and meteorological observations, known as the Subduction Experiment (Brink et al. 1995). Two, the region does not include a western boundary current – many of the previously-cited eddy-resolving adjoint model studies, such as Schröter et al. (1993) and Cong et al. (1997), were based in the Gulf Stream region. The nonlinear dynamics of the western North Atlantic are a complicating factor that we wish to avoid in first trials of state estimation with a primitive-equation eddy-resolving model.

a. Eddy-resolving model with open boundaries

The model used in the present study is the Massachusetts Institute of Technology Ocean General Circulation Model (Marshall et al. 1997a, b) with the complementary state estimation codes of the ECCO Group (Heimbach et al. 2004; Marotzke et al. 1999b). It is a z-coordinate model which employs the incompressible Navier-Stokes equations under the Boussinesq

approximation and hydrostatic balance. The goal is to obtain a best description of the oceanic circulation in this region through a least-squares fit of the model to the Subduction Experiment data for the year June, 1992, to June, 1993. All the time-dependent boundary values and initial conditions of the regional model are taken from the 2° ECCO global estimate. The National Center for Environmental Prediction (NCEP) Reanalysis daily sensible and latent heat fluxes and twice-daily surface windstresses are used as first-guess forcing fields. There are three open boundaries with sponge layers that smoothly ramp the interior field toward the boundary. Further state-of-the-art physics packages include the KPP surface boundary-layer parameterization scheme of Large et al. (1995).

The resolution of the model is $1/6^\circ$ by $1/6^\circ$, or roughly 15 *km*. With the Rossby radius of deformation between 25 and 45 *km* in this region, the model is nominally eddy-resolving. The model domain contains most of the eastern subtropical gyre of the North Atlantic (see Panel A, Figure 1). The eddy kinetic energy of the forward model is typically $50-75\%$ of TOPEX/POSEIDON observations, and $1/6^\circ$ resolution remains too coarse to fully capture the flow field.

TABLE 1.

An important element of the MIT GCM is the use of an automatic differentiation (AD) tool, here called TAF (Tranformations of Algorithms in Fortran, see Giering and Kaminski (1998)). This software permits a (semi-) automatic production of the Fortran code for the adjoint operator from that of the forward code of the MIT GCM.

b. The Northeast Atlantic least-squares problem

The eastern subtropical North Atlantic Ocean (hereafter, Northeast Atlantic Ocean) is under the influence of a large-scale pattern of negative wind stress curl (Moyer and Weller 1995) and is therefore a prime location for surface waters to subduct into the main thermocline. The Subduction Experiment was designed to study this large-scale subduction through three separate field deployments between June, 1991, and June, 1993 (see Brink et al. (1995) for detailed information). An array of five moorings observed both oceanic and meteorological fields (see

Panel B, Figure 1). The moorings collected an impressive amount of information at their point locations, but a rigorous synthesis with other forms of data has not been done.

FIG. 1.

TABLE 2.

Here, a synthesis of both data forms is possible by adding data-model misfit terms to the cost function for both the Subduction Experiment moorings and TOPEX/POSEIDON satellite altimetry, as detailed in the first five terms of Table 2. The Subduction Experiment mooring temperature, mooring meridional and zonal velocity, mean sea surface height and sea surface height anomaly are used. The form of the cost function terms is illustrated with the mooring temperature misfit term: $\Sigma^t (T(t) - T_{SubEx}(t))^T \mathbf{W}_{SubEx} (T(t) - T_{SubEx}(t))$. The weighting matrix, $\mathbf{W}_{SubEx}$, is diagonal with values that vary as a function of horizontal location, depth, and data type.

The next three terms are the climatological misfits; they constrain the estimate to the three-dimensional, monthly-varying Levitus atlas (Levitus and Boyer 1994), and the monthly-varying climatology of sea surface temperatures (Reynolds and Smith 1994). The relative weights on these terms are small because they do not represent ocean physics on all timescales, yet the climatologies still provide a major source of information.

The last eleven terms in Table 2 are control penalty terms; they constrain the control parameters to lie within a certain range of their initial guess. The control penalty terms take the place of an explicit model error term in J. Here, the controls include:

- Initial temperature and salinity
- Surface heat flux and freshwater flux (E-P-R)
- Surface wind stress
- Open boundary conditions (as formulated in Section 2).

A well-known problem with diagonal weight matrices is the emergence of small-scale noise in the estimated control fields which is unphysical because the atmosphere varies only on larger

scales. Following the work of Bennett (2002) and Lea (2001), we add an extra term to the cost function which penalizes the Laplacian of the controls: $J = \mathbf{u}(t)^T \mathbf{W}(t)\mathbf{u}(t) + (\nabla^2\mathbf{u})^T\ \mathbf{W}_1\ (\nabla^2\mathbf{u})$ where the Laplacian is an abbreviation for the discretized operator in the model grid space. As is well-known (e.g., Bennett, 1992) the effect of such numerical derivative terms is to smooth the result.

5. Search for the large-scale circulation consistent with observations

For any state estimate, the model simulation needs to be reasonable or else a relevant comparison to observations can not be made. Despite a good visual similarity between the modelled circulation and reality, the simulation has several large-scale hydrographic deficiencies. Sea surface temperature approaches $35^\circ C$ in the northern basin ($30-40^\circ N$). Overly-warm sea surface temperatures are also associated with a weakened Canaries Current in the simulation. Anomalously-warm SST is a ubiquitous problem of numerical model products including the ECCO state estimate[1]. Surface layers of the model are too warm in the summer because the seasonal mixed-layer does not deepen enough. The KPP boundary layer model parameterizes wind-stirred deepening of the mixed-layer and helps alleviate the surface model biases, but SST is still not in complete agreement with observations. Another major deficiency of the simulation is the meridional slope of the winter mixed layer base; the mixed-layer deepens to the south, reaching a depth of 220 *m*, at $22^\circ N$. In contrast, observations and climatologies alike show that the mixed-layer shoals equatorward, a crucial feature because horizontal flow across a sloping boundary leads to *subduction*, or volume flux from the mixed-layer to the main thermocline (Marshall et al. 1993; Woods 1985). The abnormally cool surface layers of the eastern subtropics between $20-30^\circ N$ are caused by large western boundary heat fluxes, and corresponding heat flux divergence near the western boundary. Adjustments to the control vector are needed to bring the model within observational uncertainty.

---

[1]Here, we have used the original ECCO state estimate from the adjoint method, 1992-1997, (Stammer et al. 2002). Later estimates (Stammer et al. 2004) do not have the same preponderance of overly-heated sea surface temperatures because of the addition of an explicit boundary layer scheme.

a. Coarse-resolution optimization

Using the quasi-Newton method of Gilbert and L émarechal (1989) and adjoint-computed gradients, (Gilbert and Lemaréchal 1989) the ocean circulation is brought within observational uncertainty in fifty iterations of the forward and adjoint models (see left panel, Figure 2). Fifty iterations is extremely efficient considering the control vector of 100,000 elements (i.e., $N_{iterations} << N_{controls}$). The successive updates of the controls further illustrates the efficiency of the optimization. The control variables quadratically converge upon the minimum of the cost function subject to the coarse resolution model (right panel, Figure 2); this is the theoretical rate of convergence for the quasi-Newton method with a parabolically-shaped cost function (Press et al. 1990). This topology is expected for a diffusive coarse-resolution ocean model. The solution for the control variables is within the prior estimated range of uncertainty. It is not surprising that the method works so well for a coarse resolution model, because it is a nearly-linear system. FIG. 2.

What does the coarse-resolution model adjust in order to fit the observations? The gradient of the cost function with respect to the controls gives the relative importance of each control. After nondimensionalizing each gradient by its data type and depth, the initial temperature and open boundary conditions are most important over the first year of integration. The memory of initial conditions extends well beyond one year – both forward model studies (Griffies and Bryan 1997) and adjoint studies (Hill et al. 2004) have shown a memory of almost ten years in the upper ocean. More specifically, the optimization shifts the open boundary southern velocity from north to south in order to accommodate more cold water advection along the coast. The optimization responds by both warming the western boundary at these latitudes, and by decreasing the westward exit flow. The optimized estimate of mixed-layer depth then shoals towards the south, and never reaches a depth greater then 170 *m*, in close accordance with observations. In summary, the overall effect of the coarse-resolution optimization is to correct for large-scale hydrographic deficiencies.

b. Application to the eddy-resolving model

Next, the control adjustments from the regional, coarse resolution state estimate are applied to the eddy-resolving model. Linear interpolation is used to change resolution of the

controls. Although the dynamics of the eddy-resolving model are different, the coarse resolution estimate is expected to have some skill in predicting the ocean observations. To investigate, two eddy-resolving model trajectories are compared: a run with zero control adjustments and another with coarse-resolution estimated controls. A comparison of the two cost function values (Table 3) shows the improvement by the coarse-resolution controls. These adjustments decrease the total observational cost function elements by 3%, primarily by bringing the model closer to the Levitus climatological temperature and Reynolds SST. Therefore, the predictions made by the coarse resolution model are useful in the eddy-resolving case. On the other hand, improvement of only 3% does not bring the eddy-resolving model into consistency with all of the observations.

TABLE 3.

Starting from coarse-resolution controls, the method of Lagrange multipliers is then applied to the eddy-resolving model. Improvement of the model trajectory comes at a slower pace due to the increased search space dimension. Nevertheless, the first-guess model run is near to the observations at the beginning, less than thirty iterations bring the large-scale state estimate within expected errors (Figure 3). The first goal is to determine if any solution exists to the least squares problem. The solid red line reaches the normalized value of $J = 1$, corresponding a root mean square error that is equal to the a priori expected error. Therefore, the optimization finds a reasonable solution to the least-squares problem.

FIG. 3.

The result is a time-evolving, three-dimensional estimate of the ocean circulation which reasonably fits a wide variety of available information and exactly follows the dynamics of the MIT General Circulation Model (Figure 4). In addition, we now have improved estimates of the initial eddy field, open boundary conditions, wind stresses, and air-sea fluxes. The state estimate is ideal for the study of the role of eddies in subduction because it is dynamically consistent and it explicitly resolves eddy-scale motions.

FIG. 4.

Much like the coarse-resolution experiment (pictured in Figure 2), adjustments to the initial conditions and open boundaries have the most influence on the ocean circulation over one year. The estimated adjustment to the initial temperature is large-scale, and has a reasonable magnitude relative to the interannual variability of the ocean (Roemmich and Wunsch 1984) (Figure 5).

FIG. 5.

The strong influence of the open boundary conditions is seen in a dye-release experiment in the forward model. Dye is constantly added at the lateral boundaries and allowed to advect and diffuse away. The result (Figure 6) is that almost half of the domain is affected by the boundaries in one year. Extrapolation suggests that the entire region would be covered by the passive tracer within three to five years. Therefore, the strong influence of the open boundary controls is expected. FIG. 6.

c. Cross-validation

A stringent posterior test is to compare the state estimate with observations that were withheld from the optimization. Cross-validation tests the model's ability to be a dynamic interpolator: Is information accurately carried away from the observational sites? In the Northeast Atlantic, there is withheld data in the form of hydrographic sections which can be compared to the estimated ocean state, and withheld meteorological mooring data which can be compared to the estimated surface controls.

WOCE hydrographic sections exist in the same region and time as the Subduction Experiment. The WOCE AR11 section along $33^{\circ}W$ was completed in November, 1992 (Pallant et al. 1995). The transect passes the western moorings at $19^{\circ}N$ and $33^{\circ}N$, but nearly 1500 *km* of ocean without hydrographic measurements separates the two. The differences between the model simulation and the state estimate are biggest in the upper 100 meters (Figure 7). Because of the changes in upper ocean structure, the mixed-layer depth is deeper by 50-100 meters in the state estimate. FIG. 7.

The state estimate visually appears to reproduce the observations to a greater extent, and error estimates confirm this assertion (Figure 8). In general, the upper layer hydrographic structure is significantly improved in the state estimate relative to the withheld WOCE hydrography; data-model misfits are no larger than $1-2\ ^{\circ}C$. The unconstrained model simulation does not transport enough heat down into the water column, and hence, is $4-5\ ^{\circ}C$ warmer than the observations at the surface. This success of the model in reproducing withheld data lends confidence to the state estimate throughout the entire domain, even away from sites of observations. Although the state estimate is an improvement, systematic errors do remain. Estimated surface temperature is as much as $1\ ^{\circ}$ warmer than observed, yet is erroneously cold at the base of the mixed layer

(50 – 100 meters depth). The modelled physics of the mixed layer lead to this deficiency. FIG. 8.

Note: Could add a section about the surface heat flux adjustments. The Subduction Experiment found that the net heat flux into the region was not zero, as previously assumed and as described by NCEP. The heat flux adjustments here are consistent with the mooring observations in the regional mean.

d. Open boundary adjustments

Note: could add a paragraph here. Show how open boundary adjustments fix the Azores Current. Also show that the o.b. adjustments seems to be physically reasonable - i.e., thermal wind balance.

6. Tracking eddies

After finding a state estimate consistent with the large-scale observational signal, the next question is whether a model can be constrained to both the large and small-scale data signal. If the answer is affirmative, then individual eddies can be tracked, insofar as they are observed. The technical implementation of this new problem is very similar to the previous experiment, only the observational weights must be increased in order to correspond to the decrease in the expected errors (see Table 4). Although the mathematical transformation between the two problems is straightforward, the new least-squares problem poses a more stringent test than the original. Finding the model solution that fits the large scale signal alone is roughly equivalent to the study of Köhl and Willebrand (2002), where statistical characteristics were constrained. Tracking individual eddy trajectories is a more demanding task, and one in which the existence of any solution can not be determined a priori.

TABLE 4.

Optimization of the full cost function with stringent weights frequently stalls in control space. Changing the weights usually results in further improvements of the model trajectory. One particular change is to only weight the mooring terms in the cost function. This is a somewhat simpler test for the method: Fit the full observational signal of the moorings. In this case, the

data-model misfit at the mooring sites decreases from 7.6 σ to 1.8 σ where σ is the expected error (Figure 9). The gradient information looks plausible and a slow rate of convergence is kept. Approximately 150 iterations of the forward-adjoint model are probably needed for complete convergence. Physically, the state estimate time-series at the Central mooring resembles the results of Spall et al. (2000); vertical diffusion transfers the warm summertime surface temperature to greater depth after a few months.

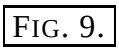

a. Estimates of the initial eddy field

What control adjustments allow eddies to be tracked away from the moorings? Analysis of the adjoint-calculated gradient shows two bands of increased sensitivity to the cost function: the Azores Current and the North Equatorial Current. Previous studies, including Gill et al. (1974), have shown the basic state North Equatorial Current to be baroclinically-unstable. The Azores Current is also a source of eddy energy, as seen in the TOPEX/POSEIDON altimeter measurement. Baroclinic instability is theorized to increase the sensitivity of these regions (Galanti and Tziperman 2003), because eddies can grow and transport information away from their formation site. In the optimization here, small perturbations in the initial conditions lead to large changes in the eddy field at later times (Figure 10). Furthermore, the mooring contribution of the cost function is most sensitive to initial temperature.

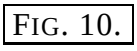

b. Pitfalls in eddy-resolving estimation

Figure 3 shows a nearly monotonic decrease of the cost function with iteration. However, many intermediate steps failed due to numerical and physical problems; they are catalogued in this section. Special cases arise when the gradient computed by the eddy-resolving adjoint model is less useful. The adjoint of the KPP boundary layer model is troublesome in shallow water and at depth due to the shear instability term. The solution here is to only use KPP in the forward model in the boundary layer, and to avoid simulating the shelf circulation. Also, the Hessian information calculated from the gradients is frequently not useful. For this reason, a steepest descent method periodically works better than the full quasi-Newton method. This is a clue that the underlying cost function topology is not well-represented by a paraboloid, and instead the

topology is irregular. Most of these problems, now known, can be avoided in future by choosing a different optimization technique.

7. Summary

Careful formulation of the open boundary controls is necessary to avoid ill-conditioning of the search space. In addition, a multiscale method was employed to constrain the large-scale circulation without explicitly fitting the eddy-scale signal. Based on this work, there is no fundamental obstacle to constraining an eddy-resolving model to observations in the Northeast Atlantic Ocean. Here, a state estimate consistent to the large-scale signal in all observations is found. Furthermore, small-scale motions observed by the moorings are capably reproduced by the state estimate. Individual eddies are tracked insofar as they influence the mooring sites. The search for these state estimates is helped by the following two conditions. One, the eastern subtropical gyre is more quiescent than the western boundary of the basin, where strongly nonlinear features exist. Two, a coarse-resolution model skillfully simulates much of the large-scale ocean circulation, and can be used to eliminate major biases in an eddy-resolving model.

a. Future Work

The methodology of state estimation will be tested in the case of multi-year and decadal eddy-resolving estimates. Global eddy-resolving models will serve as a test because of differing physical regimes in different regions. Western boundary currents, open ocean deep convection, and sea-ice formation are nonlinear processes and probably represent necessary components of a realistic global ocean model. In the face of these strong nonlinear features, the usefulness of adjoint-computed gradients has been questioned, and this study can not prove that a simple formulation of the method of Lagrange multipliers will be successful everywhere. However, the techniques used here, such as the multiscale form of the cost function with a coarse-resolution twin model, suggest that there are still simple ideas to try with eddy-resolving state estimation in global models or in more nonlinear regions.

Acknowledgments.

REFERENCES

Bennett, A., and P. E. Kloeden, 1981: The ill-posedness of open ocean models. *J. Phys. Oceanogr.*, **12**, 1004–1018.

Bennett, A. F., 1992: *Inverse methods in physical oceanography*. Cambridge Monographs, Cambridge University Press.

Bennett, A. F., 2002: *Inverse Modeling of the Ocean and Atmosphere*. Cambridge University Press, 234 pp.

Brink, N. J., K. A. Moyer, R. P. Trask, and R. A. Weller, 1995: The Subduction Experiment: Mooring field program and data summary. Woods Hole Oceanographic Institution, Tech. rep., woods Hole Oceanographic Institution, *Tech. rep.*

Cong, L. Z., M. Ikeda, and R. M. Hendry, 1998: Variational assimilation of geosat altimeter data into a two-layer quasi-geostrophic model over the newfoundland ridge and basin. *Journal of Geophysical Research-oceans*, **103**(C4), 7719–7734.

Ferron, B., and J. Marotzke, 2003: Impact of 4D-variational assimilation of WOCE hydrography on the meridional circulation of the Indian Ocean. *Deep Sea Research Part II: Topical Studies in Oceanography*, **50**, 2005–2021.

Fu, L.-L., E. Christensen, C. A. Yamarone, M. Lefebvre, Y. Menard, M. Dorrer, and P. Escudier, 1994: TOPEX/POSEIDON mission overview. *J. Geophys. Res.*, **99 (C12)**, 24,369–24,381.

Fu, L.-L., B. Cheng, and B. Qiu, 2001: 25-day period large-scale oscillations in the Argentine Basin revealed by the TOPEX/Poseidon altimeter. *J. Phys. Oceanogr.*, **31**, 506–516.

Fukumori, I., 2002: A partitioned kalman filter and smoother. *Monthly Weather Review*, **130**(5), 1370–1383.

Galanti, E., and E. Tziperman, 2003: A mid-latitude ENSO teleconnection mechanism via baroclinically unstable Long Rossby Waves. *J. Phys. Oceanogr.*, **33**, 1877–1888.

Gebbie, G., 2004: Subduction in an eddy-resolving state estimate of the Northeast Atlantic Ocean, Ph.D. thesis, Massachusetts Institute of Technology / Woods Hole Oceanographic Institution Joint Program in Oceanography.

Gebbie, G. A., 2005: Is eddy subduction important in the Northeast Atlantic Ocean? In preparation.

Giering, R., and T. Kaminski, 1998: Recipes for adjoint code construction. *ACM Trans. Math. Software*, **24 (4)**, 437–474.

Gilbert, J. C., and C. Lemaréchal, 1989: Some numerical experiments with variable-storage quasi-Newton algorithms. *Math. Program.*, **45**, 407–435.

Gill, A. E., J. S. A. Green, and A. J. Simmons, 1974: Energy partition in the large-scale ocean circulation and the production of mid-ocean eddies. *Deep-Sea Res.*, **21**, 499–528.

Griffies, S. M., and K. Bryan, 1997: Predictability of North Atlantic interdecadal variability. *Science*, pp. 181–184.

Hall, M. C. G., D. G. Cacuci, and M. E. Schlesinger, 1982: Sensitivity analysis of a radiative-convective model by the adjoint method. *J. Atmos. Sci.*, **39**, 2038–2050.

Heimbach, P., C. Hill, and R. Giering, 2004: An efficient exact adjoint of the parallel mit general circulation model, generated via automatic differentiation. *Future Generation Computer Systems (FGCS)*, **in press**. Hei-eta:02b,in press.

Hill, C., V. Bugnion, M. Follows, and J. Marshall, 2004: Evaluating carbon sequestration efficiency in an ocean circulation model by adjoint sensitivity analysis. *J. Climate*. Submitted.

Kalnay, E., and coauthors, 1996: The NCEP/NCAR 40-year reanalysis project. *Bull. Amer. Meteor. Soc.*, pp. 77,431–77,437.

Köhl, A., and J. Willebrand, 2003: Variational assimilation of SSH variability from TOPEX/POSEIDON and ERS1 into an eddy-permitting model of the North Atlantic. *J. Geophys. Res.*, **108 (C3)**, 3092.

Large, W., J. C. McWilliams, and S. C. Doney, 1994: Oceanic vertical mixing: A review and model with nonlocal boundary layer parameterization. *Rev. of Geophys.*, **32**, 363–403.

Lea, D., 2001: Joint assimilation of sea surface temperature and sea surface height, Ph.D. thesis, University of Oxford.

Lea, D. J., M. R. Allen, and T. W. N. Haine, 2000: Sensitivity analysis of the climate of a chaotic system. *Tellus*, **52A**, 523–532.

Levitus, S., and T. Boyer, 1994: World ocean atlas 1994 volume 4: Temperature. U.S. Department of Commerce, NOAA Atlas NESDIS 4.

Levitus, S., R. Burgett, and T. Boyer, 1994: World ocean atlas 1994 volume 3: Nutrients. U.S. Department of Commerce, NOAA Atlas NESDIS 3.

Marchesiello, P., J. C. McWilliams, and A. Shchepetkin, 2001: Open boundary conditions for long-term integration of regional oceanic models. *Ocean Modelling*, **3**, 1–20.

Marotzke, J., R. Giering, K. Q. Zhang, D. Stammer, C. Hill, and T. Lee, 1999a: Construction of the adjoint MIT ocean general circulation model and application to Atlantic heat transport sensitivity. *J. Geophys. Res.*, **104**, 529–547.

Marotzke, J., R. Giering, K. Q. Zhang, D. Stammer, C. Hill, and T. Lee, 1999b: Construction of the adjoint mit ocean general circulation model and application to Atlantic heat transport sensitivity. *J. Geophys. Res.*, **104**(C12), 29,529–29,547.

Marshall, J., A. Adcroft, C. Hill, L. Perelman, and C. Heisey, 1997a: Hydrostatic, quasi-hydrostatic and nonhydrostatic ocean modeling. *J. Geophys. Res.*, **102, C3**, 5,753–5,766. Mars-eta:97b.

Marshall, J., C. Hill, L. Perelman, and A. Adcroft, 1997b: Hydrostatic, quasi-hydrostatic and nonhydrostatic ocean modeling. *J. Geophys. Res.*, **102, C3**, 5,733–5,752. Mars-eta:97a.

Marshall, J. C., A. J. G. Nurser, and R. G. Williams, 1993: Inferring the subduction rate and period over the North Atlantic. *J. Phys. Oceanogr.*, **23**, 1315–1329.

Morrow, R., and P. Demey, 1995: Adjoint assimilation of altimetric, surface drifter, and hydrographic data in a quasi-geostrophic model of the azores current. *Journal of Geophysical Research-oceans*, **100**(C12), 25,007–25,025.

Moyer, K. A., and R. A. Weller, 1995: Observations of surface forcing from the Subduction Experiment: A comparison with global model products and climatological datasets. *J. Climate*, **10**, 2725–2742.

Oliger, J., and A. Sundström, 1978: Theoretical and practical aspects of some initial value boundary in fluid dynamics. *SIAM J. App. Math.*, **35**, 419–446.

Pallant, J. S., F. B. Bahr, T. M. Joyce, J. P. Dean, and J. R. Luyten, 1995: Subduction in the subtropical gyre: Seasoar cruises data report. Woods Hole Oceanographic Institution, *Tech. rep.*

Pond, S., and G. L. Pickard, 1983: *Introductory Dynamical Oceanography*. Pergamon Press.

Press, W. H., B. P. Flannery, S. A. Teukolsky, and W. T. Vetterling, 1990: *Numerical Recipies*. Cambridge University Press.

Reynolds, R. W., and T. M. Smith, 1994: Improved global sea surface temperature analysis using optimum interpolation. *J. Climate*, **7**, 929–948.

Roemmich, D., and C. Wunsch, 1984: Apparent change in the climatic state of the deep North Atlantic Ocean. *Nature*, **307**, 447–450.

Schroter, J., and C. Wunsch, 1986: Solution of nonlinear difference ocean models by optimization methods with sensitivity and observational strategy analysis. *J. Phys. Oceanogr.,* **16**, 1855–1874.

Schröter, J., U. Seiler, and M. Wenzel, 1993: Variational assimilation of GEOSAT data into an eddy-resolving model of the Gulf Stream Extension area. *J. Phys. Oceanogr.*, **23**, 925–953.

Sirkes, Z., E. Tziperman, and C. W. Thacker, 1996: Combining data and a global primitive equation ocean general circulation model using the adjoint method. *Modern approaches to data assimilation in ocean modeling, Malanotte-Rizzoli, P. Ed., Elsevier*.

Stammer, D., C. Wunsch, R. Giering, C. Eckert, P. Heimbach, J. Marotzke, A. Adcroft, C. N. Hill, and J. Marshall, 2002: The global ocean circulation during 1992-1997, estimated from ocean observations and a general circulation model. *J. Geophys. Res.*, **107 (C9)**, 3118.

Stammer, D., C. Wunsch, R. Giering, C. Eckert, P. Heimbach, J. Marotzke, A. Adcroft, C. Hill, and J. Marshall, 2003: Volume, heat and freshwater transports of the global ocean circulation 1993 –2000, estimated from a general circulation model constrained by WOCE data. *J. Geophys. Res.*, **108(C1)**, 3007. Sta-eta:03.

Stammer, D., K. Ueyoshi, A. Kohl, W. G. Large, S. A. Josey, and C. Wunsch, 2004: Estimating air-sea fluxes of heat, freshwater, and momentum through global ocean data assimilation. *Journal of Geophysical Research-oceans*, **109**(C5).

Stevens, D. P., 1991: The open boundary condition in the United Kingdom fine-resolution Antarctic model. *J. Phys. Oceanogr.*, **21**, 1494–1499.

Talagrand, O., 1997: Assimilation of observations: An introduction. *J. Met. Soc. Jpn.*, **75**, 191–209.

Tanguay, M., P. Bartello, and P. Gauthier, 1995: Four-dimensional data assimilation with a wide range of scales. *Tellus*, **47A**, 974–997.

Woods, J. D., 1985: The physics of thermocline ventilation. *Coupled Ocean-Atmosphere Models*, J. C. J. Nihoul, Ed., pp. 543–590.

Wunsch, C., 1996: *The Ocean Circulation Inverse Problem*. Cambridge University Press.

Wunsch, C., and A. E. Gill, 1976: Observations of equatorially trapped waves in Pacific sea level variations. *Deep-Sea Res.*, **23**, 371–390.

Zang, X., and C. Wunsch, 2001: Spectral description of low-frequency oceanic variability. *J. Phys. Oceanogr.*, **31**, 3073–3095.

Printed February 28, 2005.

Figure Captions

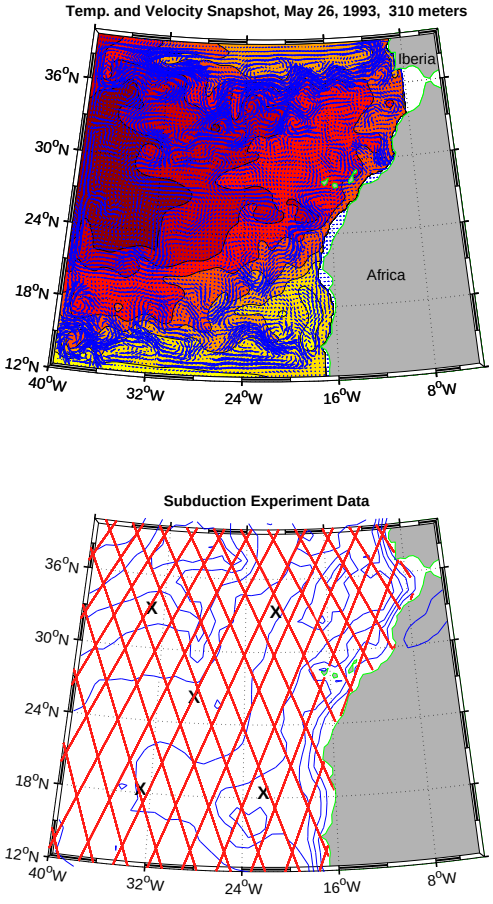

FIG. 1. *Left*: Snapshot of the $1/6^\circ$ model temperature and velocity fields at 310 meters depth. Temperature has 1° contour intervals from $15^\circ C$ to $21^\circ C$. The full model domain and three open boundaries are shown. This snapshot represents our first guess at the true ocean state on June 1, 1993. The model was started one year earlier, June 1, 1992. *Right*: The Subduction Experiment was an intensive field experiment designed to study the subduction of fluid from the mixed layer into the main thermocline. This study uses 5 moorings (marked by "X") with temperature, velocity, and meteorological observations. TOPEX/Poseidon altimetry (marked by bold, solid tracks) is also used here. The thin solid lines are depth contours with an interval of 1000 *m*.

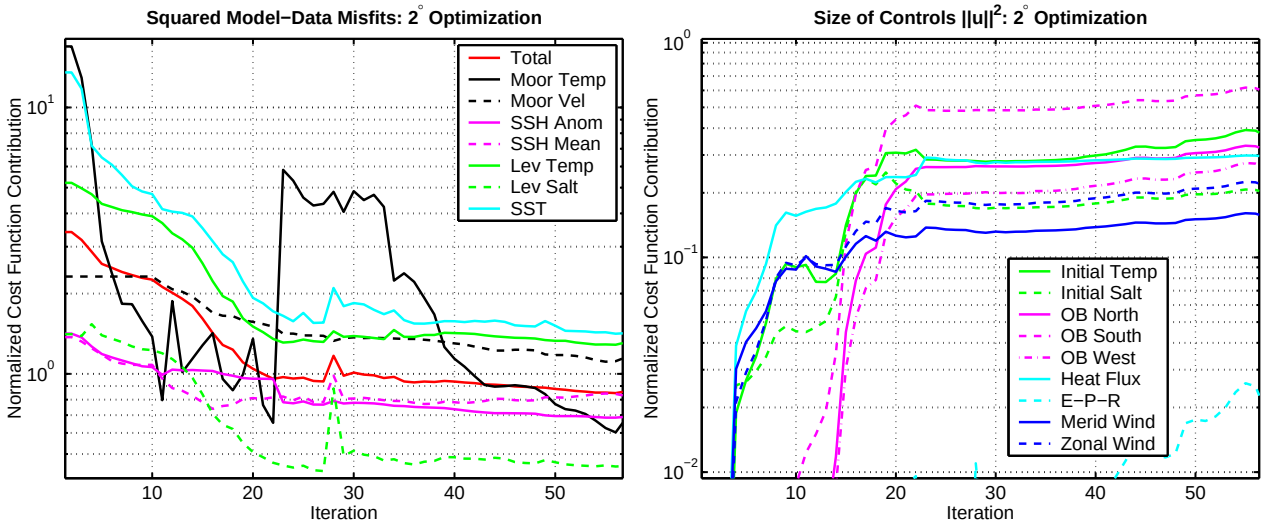

FIG. 2. *Left panel*: Normalized model-data misfit as a function of iteration of the search method. A value of 1 (10^0) is expected. Irregularities are caused by improvements and changes in the numerical code; for example, the increase in the mooring temperature misfit occurred when the data-model mapping was improved in the numerical code.*Right panel*: The size of the control adjustments, $||u||^2$, for the same experiment.

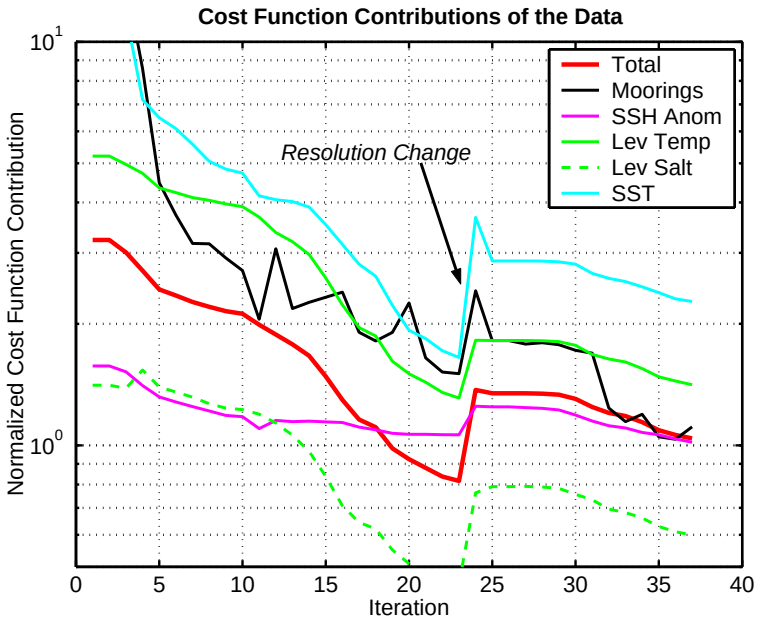

FIG. 3. Normalized model-data misfit as a function of iteration of the search method for the coarse and eddy-resolving optimization. A value of 1 (10^0) is expected.

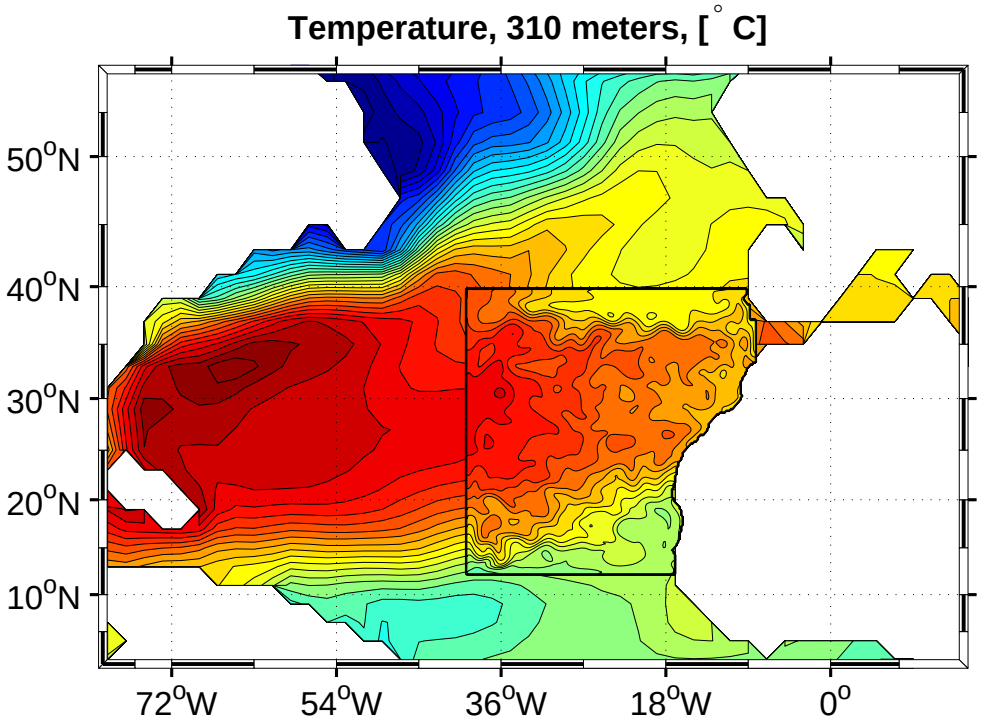

FIG. 4. Nested view of the $1/6^\circ$ regional state estimate inside the 2° ECCO state estimate. Potential temperature at 310 meters depth, with a contour interval of $1^\circ C$, is shown. The boundary between the two estimates (*thick black line*) is discontinuous in temperature because of the open boundary control adjustments.

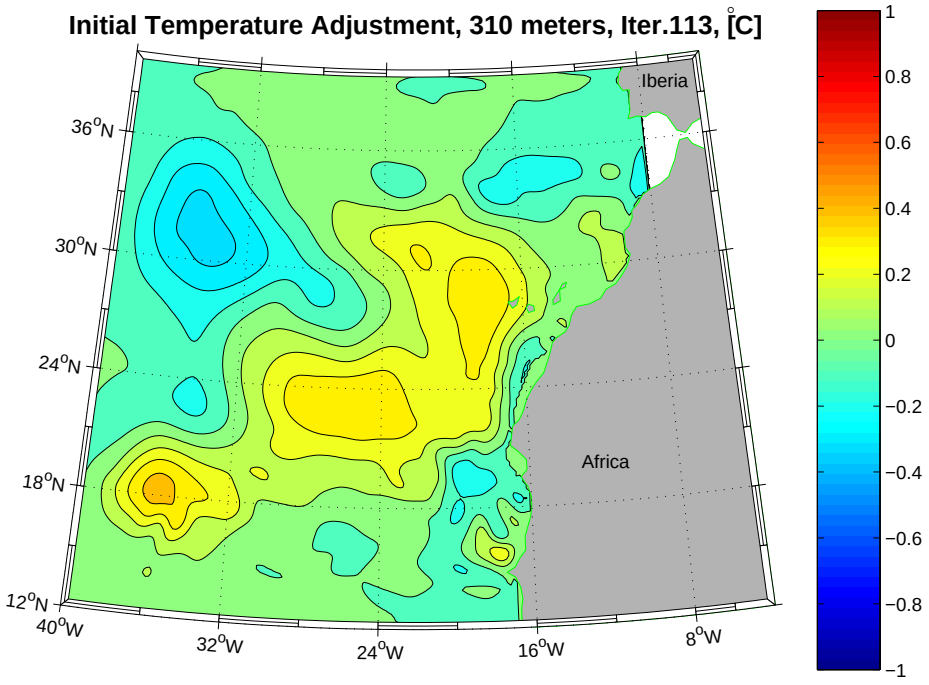

FIG. 5. Initial temperature adjustment to bring the eddy-resolving estimate into consistency with the large-scale observational signal.

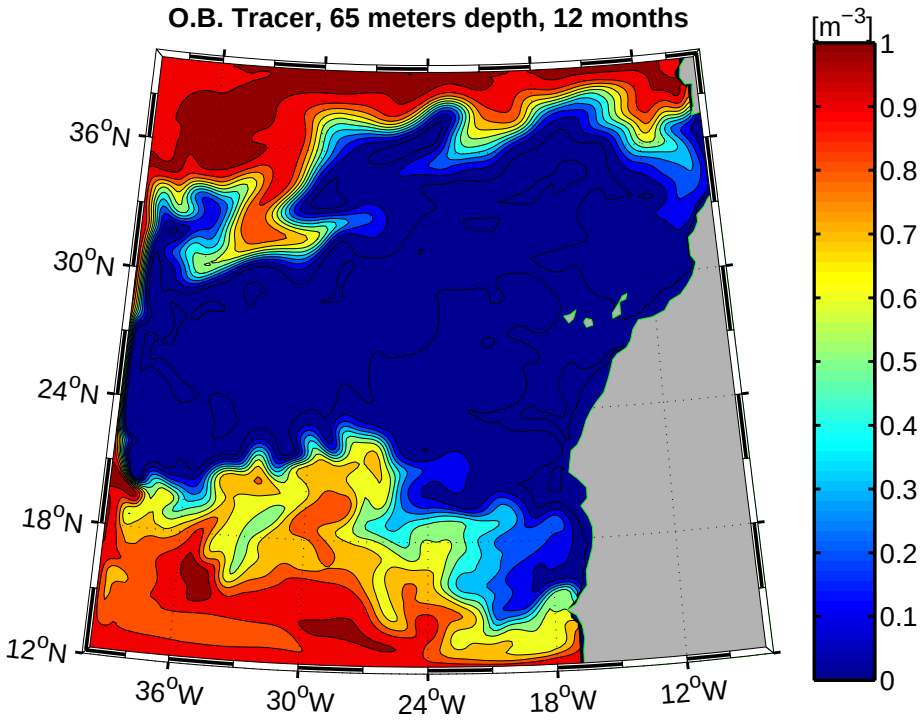

FIG. 6. Tracer concentration $[m^{-3}]$ at 65 meters depth of a passive dye constantly released from the open boundaries with concentration 1 m^{-3}. This snapshot is taken one year after the initial release of dye. The contour interval is 0.1 m^{-3}.

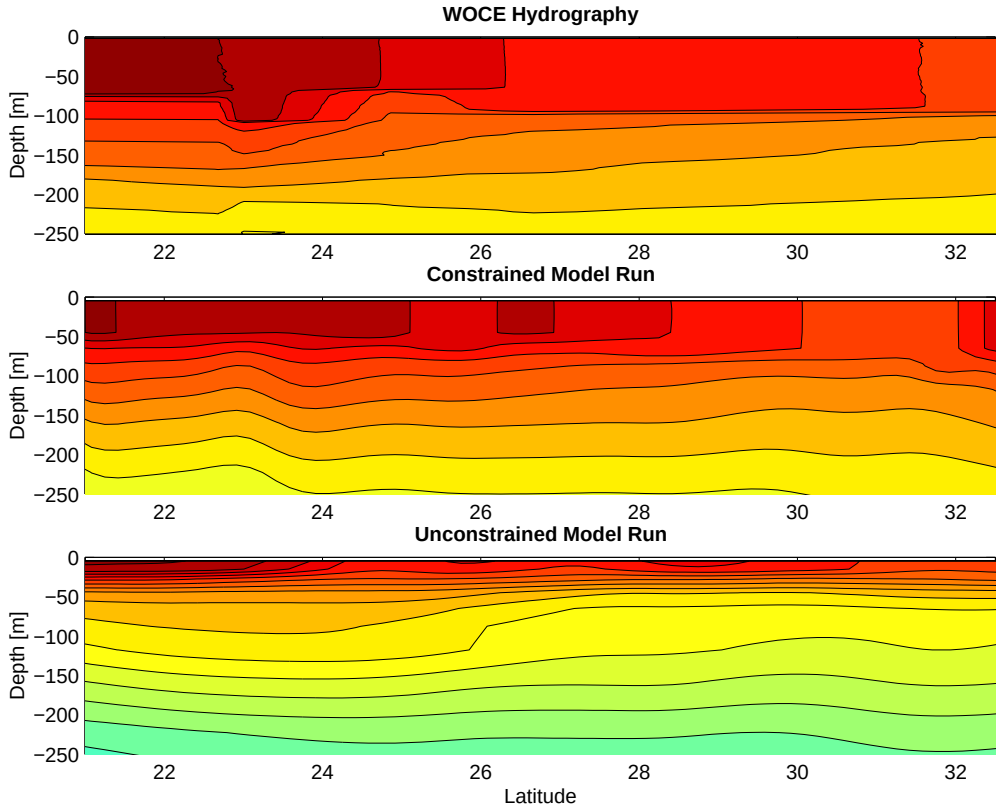

FIG. 7. Meridional sections of potential temperature along the WOCE AR11 line (33°*W*) in November, 1992. *Top panel*: Observations from WOCE (courtesy of T. Joyce). *Middle panel*: Constrained model estimate. *Lower panel*: Unconstrained model simulation.

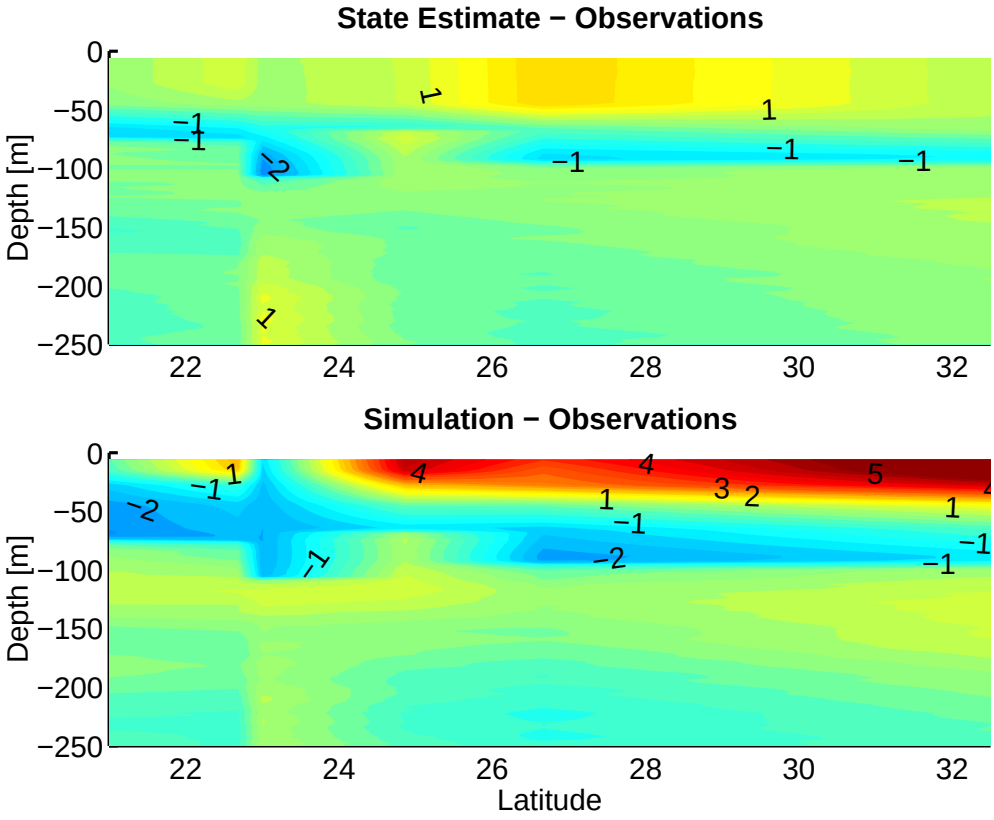

FIG. 8. Error in potential temperature along the meridional WOCE AR11 line (33°*W*) in November, 1992. *Upper panel*: Difference between the state estimate (constrained model) temperature and observations. *Lower panel*: Difference between model simulated temperature (no data constraint) and observations.

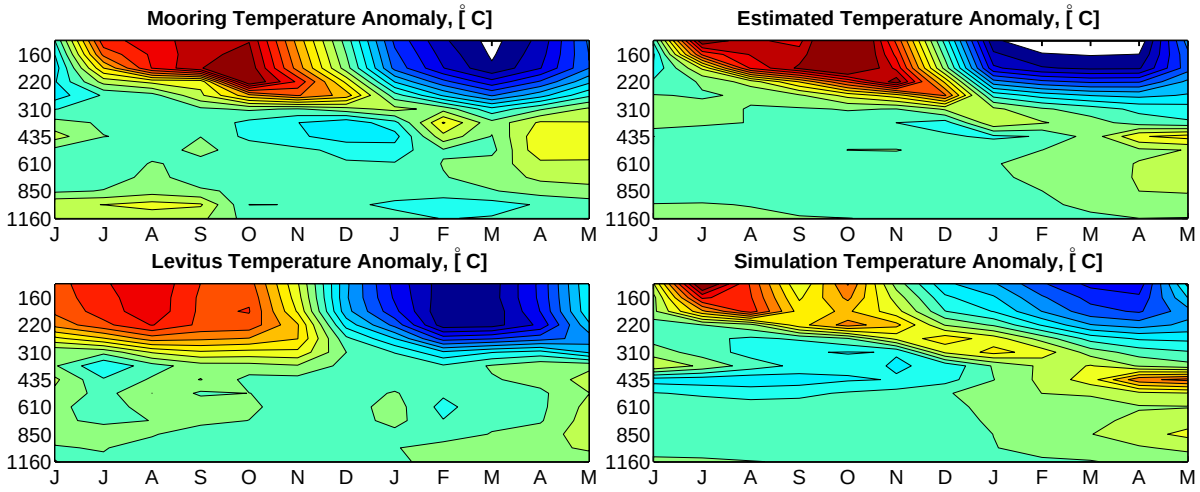

FIG. 9. Four depth-time diagrams of potential temperature at the Central Mooring site from June 1, 1992, to June 1, 1993. *Top left*: Mooring observations, *bottom left*: Levitus climatology, *top right*: Constrained model estimate, *bottom right*: Unconstrained model simulation. The constrained model estimate accurately depicts the timing of and magnitude of the seasonal cycle, unlike the unconstrained model.

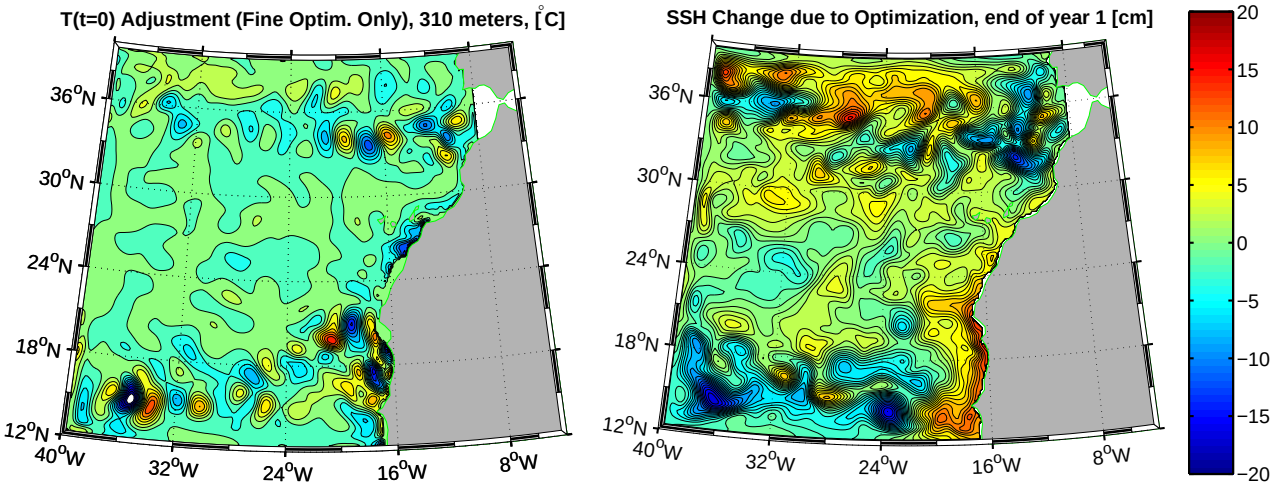

FIG. 10. *Left*: Initial temperature adjustment from the optimization of the small-scale observational signal. *Right*: Rearrangement of the sea surface height field after one year by the initial temperature adjustment.

Tables

	$\mathbf{2}^{\circ}$	$\mathbf{1/6}^{\circ}$
Horizontal Resolution	$(167-218)$ *km* x 222 *km*	$(14.2-18.2)$ *km* x 18.5 *km*
Grid Points	20 x 16 x 23 vertical levels	192 x 168 x 23 vertical levels
Time Step	3600 s = 1 hr.	900 s = 15 min.
Lap. Horiz. Viscosity	$5\text{x}10^{4}\ m^2/s$	0
Lap. Horiz. Diffusivity	$1\text{x}10^{3}\ m^2/s$	0
Biharmonic Horiz. Vis./Diff.	0	$2\text{x}10^{11}\ m^4/s$
Vertical Viscosity	$1\text{x}10^{-3}\ m^2/s$	$1\text{x}10^{-3}\ m^2/s$
Vertical Diffusivity	$1\text{x}10^{-5}\ m^2/s$	$1\text{x}10^{-5}\ m^2/s$
Reynolds Number	≈ 1	≈ 25
State Vector	1.70 x 10^4 elements	3.14 x 10^6 elements
Control Vector	9.11 x 10^4 elements	5.49 x 10^6 elements
Observations	1.28 x 10^7 elements	1.28 x 10^7 elements
Model Input	7.68 x 10^5 forcing elements	7.98 x 10^7 forcing elements
Model Output	1.50 x 10^8 estimated elements	1.09 x 10^{11} estimated elements
Processors	1 processor	24-48 processors
Computational Time	2 cpu hours/iteration	400 cpu hours/iteration
Search Iterations	$\approx$ 40 iterations	$\approx$ 120 iterations
Total Computer Time	$\approx$ 80 hours (2.3 days)	$\approx$ 50,000 hours (5.7 years)

TABLE 1. Coarse and eddy resolution state estimation

Observational Terms	**Freq.**	#	$< n^T n >^{1/2}$ (2°)	$< n^T n >^{1/2}$ $(1/6^\circ)$	**References**	**Notes**
Mooring Temperature	mon. avg.	12	$XX\ ^\circ C$	$XX\ ^\circ C$	Brink et al. (1995)	interpolated to model levels
Mooring Zonal Velocity	”	”	$XX\ m/s$	$XX\ m/s$	”	”
Mooring Meridional Velocity	”	”	$XX\ m/s$	$XX\ m/s$	”	”
TOPEX/POSEIDON anomaly	daily	365	$XX\ cm$	$XX\ cm$	Fu et al. (1994), Tai and Kuhn (1995)	pointwise
TOPEX/POSEIDON mean		1	$XX\ cm$	$XX\ cm$	Lemoine et al. (1997)	relative to geoid, gridded
Climatological Terms						
Levitus Temperature	monthly	12	$XX\ ^\circ C$	$XX\ ^\circ C$	Levitus et al. (1994)	interpolated to model levels
Levitus Salinity	”	”	XX	XX	”	”
Reynolds SST	monthly	12	$XX\ ^\circ C$	$XX\ ^\circ C$	Reynolds and Smith (1994)	
Initial Conditions						
ECCO Temperature	June 1, 1992	1	$XX^\circ C$	$XX^\circ C$	Stammer et al. (2002)	identical grid
ECCO Salinity	”	”	XX	XX	”	”
Surface Forcing						
NCEP Net Heat Flux	every 10 days	37	$XX\ W/m^2$	$XX\ W/m^2$	Kalnay al. (1996)	NCEP Reanalysis Project
NCEP E-M-R	”	”	$XX\ m/s$	$XX\ m/s$	”	fwd model forced daily
NCEP Wind Stress	”	”	$XX\ N/m^2$	$XX\ N/m^2$	”	fwd model forced 2x day
Open Boundary Terms						
ECCO Temperature	monthly	12	$XX\ ^\circ C$	$XX\ ^\circ C$	Stammer et al. (2002)	
ECCO Salinity	”	”	XX	XX	”	
ECCO Tangential Velocity	”	”	$XX\ m/s$	$XX\ m/s$	”	
ECCO Normal Velocity	”	”	$XX\ m/s$	$XX\ m/s$	”	
Thermal Wind Deviation	”	”	$XX\ m/s$	$XX\ m/s$	Pond and Pickard (1983)	assume Ro = 0.1

TABLE 2. Terms of the cost function. The first column introduces nineteen types of terms in the cost function, which are further divided into five main categories (i.e., *Observational, Climatological, Initial Conditions, etc.*). The second column, *Freq.*, refers to the frequency of comparison between the model and prior information. The third column gives the total number of terms in time per cost function type. The fourth column gives the average expected error in the 2° optimization problem, which is used for calculating weights. The fifth column is the same information, but for the eddy-resolving problem. *References* are given for the data source or error estimates. The *Notes* give some extra information regarding the cost function evaluation.

Cost Function Element	Simulation	Coarse-resolution Controls
Mooring Temperature	2.24	2.01
Mooring Velocity	0.98	1.02
SSH Anomaly	1.32	1.24
SSH Mean	1.01	0.94
Levitus Temperature	2.06	1.82
Levitus Salinity	0.76	0.76
Reynolds SST	6.30	3.67

TABLE 3. Squared misfit of cost function terms normalized by their expected value. The expected value is computed by treating all small-scale motions as noise. Here, the comparison is made between two integrations of the eddy-resolving model, one with zero control adjustments (*Simulation*), the other with controls estimated from the coarse-resolution model (*Coarse-resolution controls*).

Observational Terms	**Freq.**	#	$<n^T n>^{1/2}$ (2°)	$<n^T n>^{1/2}$ (1/6°)	**References**	**Notes**
Mooring Temperature	mon. avg.	12	$XX°C$	$XX°C$	Brink et al. (1995)	interpolated to model levels
Mooring Zonal Velocity	”	”	$XX\ m/s$	$XX\ m/s$	”	”
Mooring Meridional Velocity	”	”	$XX\ m/s$	$XX\ m/s$	”	”
Initial Conditions						
ECCO Temperature	June 1, 1992	1	$XX\ °C$	$XX\ °C$	Stammer et al. (2002)	identical grid
ECCO Salinity	”	”	XX	XX	”	”
Surface Forcing						
NCEP Net Heat Flux	every 10 days	37	$XX\ W/m^2$	$XX\ W/m^2$	Kalnay al. (1996)	NCEP Reanalysis Project
NCEP E-M-R	”	”	$XX\ m/s$	$XX\ m/s$	”	fwd model forced daily
NCEP Wind Stress	”	”	$XX\ N/m^2$	$XX\ N/m^2$	”	fwd model forced 2x day
Open Boundary Terms						
ECCO Temperature	monthly	12	$XX\ °C$	$XX\ \circ C$	Stammer et al. (2002)	
ECCO Salinity	”	”	XX	XX	”	
ECCO Tangential Velocity	”	”	$XX\ m/s$	$XX\ m/s$	”	
ECCO Normal Velocity	”	”	$XX\ m/s$	$XX\ m/s$	”	
Thermal Wind Deviation	”	”	$XX\ m/s$	$XX\ m/s$	Pond and Pickard (1983)	assume Ro = 0.1

TABLE 4. Terms of the cost function for the “eddy-tracking” problem. The layout of the table follows Table 2.